International Journal of Chemical Studies

P-ISSN: 2349–8528
E-ISSN: 2321–4902
IJCS 2017; 5(4): 1890-1894

Received: 12-05-2017
Accepted: 14-06-2017

Jean-Pierre Sagou Sagou
Laboratory of Materials Inorganics Chemistry, Felix Houphouet BOIGNY University, Abidjan, Ivory Coast 22 BP 582 Abidjan 22, Abidjan, Côte d'Ivoire

Correspondence
Jean-Pierre Sagou Sagou
Laboratory of Materials Inorganics Chemistry, Felix Houphouet BOIGNY University, Abidjan, Ivory Coast 22 BP 582 Abidjan 22, Abidjan, Côte d'Ivoire

Colloidal stability and aggregation of functionalized carboxymethyldextran in presence of copper

Jean-Pierre Sagou Sagou

Abstract
The turbidity profil and the evolution of size and structure during the aggregation of carboxymethyldextran in presence of copper has been examined in saline water througth turbidity and light scattering measurements. These two completely independent techniques allowed to determine experimental destabilization conditions of colloidal suspension. A critical coagulation ratio has been observed. The aggregated particles remain stable below this equilibrum point whereas an aggregates destabilization process occurs and leads to a gelatinous and homogeneous deposit beyond this ratio.

Keywords: Carboxymethyldextran, copper, Turbidity, Light Scattering, Aggregation.

Introduction
Human activities are often responsible of the emission of a large fraction of heavy metals to the soils [1-4]. One of the technologies used for the removal of these highly hazardous contaminants from soils is based on phytoremediation [5-9] which uses plants hyperaccumulating metals. These assimilate metals from soils and transfer them to aerial parts that can be harvested and treated [10, 11]. However, this process depends on the mechanisms that govern the absorption of metals by the roots. Indeed, the transfer of metals from soil matrix to plant roots occurs through the so-called mucilage, which is the biofilm built by microorganisms around the roots from exsudated glucidic material. The chemical interactions between metal ions and polysaccharides, and their influence on the conformational properties of the macromolecules are of great importance in the understanding of biodisponibility and phytotoxicity of metals. Early studies were focused on the identification of the molecular mechanisms underlying the interactions between an anionic polysaccharide and divalent cadmium (Cd^{2+}) and calcium (Ca^{2+}) ions. We studied at the local scale (chemical), the complexation mechanism, the structure of the formed complex, the thermodynamics of the complexation [12]. At the macromolecular scale (intramolecular), we analyzed the role of complexation on electrostatic interactions and thus on the conformational, thermodynamic and electrocinetic properties of the polysaccharide [12-14]. Knowing that the technologies used for elimination of heavy metals from the environment are also based on a whole range of physicochemical and interfacial processes including precipitation [15, 16], ion exchange [17-19], adsorption [20, 21], membrane filtration [22, 23], coagulation [24-27], we have undertaken, in the framwork of the present work, to study at intermolecular scale point of view the aggregation process of polysaccharides in presence of heavy metals. At this end, we have adopted an experimental and analytical approach. This approach will consist to an acquisition of experimental data by pointing out the conditions of colloidal stability, the coagulation of polysaccharides by metals, and the structure of the aggregates. Carboxymethyldextran is chosen as polysaccharide. The selected heavy metal is copper since it is a metal which migrates little in depth except under special conditions of drainage or in a very acid medium and is preferentially fixed on the organic matter, iron oxides, Manganese, carbonates and mineralogical clays.

Material and methods

Material

Reagents. The chemicals listed below were from analytical grades and used as received: NaCl from Prolabo (Merck, USA); HNO_3, NaOH, $ClCH_2COOH$, {$CuCl_2$, $2H_2O$} from Aldrich (St. Quentin Fallavier, France). Ultrapure Milli-Q water was used in the preparation of solutions.

Carboxymethyldextran. Native Dextran T500, a biopolymer of bacterial origin from Amersham Biosciences (Uppsala, Sweden), was chemically functionalized by carboxymethyl grafting under alkaline conditions as described elsewhere [12, 28,29] yielding carboxymethyldextran (CMD).

Characterization. The degree of substitution (DS), i.e. the amount of carboxymethyl groups per 100 glucopyranosidic units of the synthesized CMD, was determined according two ways: potentiometric titration at ionic strength of 100 mM NaCl and pH7 (complete dissociation of the carboxylic sites) and conductometric titration in CMD suspension without salt, which provide the same values. The hydrodynamic diameter (D) of native Dextran T500 and the synthesized CMD, and their weight-average molar mass (Mw) were measured at 25.0 ± 0.1 C using a Zetasizer Nano ZS instrument (He–Ne red laser (633 nm), Malvern Instruments) and the multi angle laser light scattering coupled to steric exclusion chromatography.

Table 1 : Values of the degree of substitution (DS), hydrodynamic diameter (D) and weight-average molar mass (Mw) of the Native Dextran T500 and CMD at pH 7 in 100 mM NaCl.

Polymer	DS (%)		D (nm)	Mw (g/mol)
Dextran T500	-	494,200	40	494,200
CMD	37	630,000	50	630,000

Sample preparation. Due to the importance of the process of dispersion in flocculation studies, polysaccharide solutions were prepared 24 h prior to experiments in NaCl electrolyte solution and stored at 4°C to ensure complete dispersion of polymers. It should be noted that these suspensions were dispersed away from light to prevent the proliferation of algae or bacteria. Stock solutions of metallic Cu^{2+} were obtained by dissolution of $CuCl_2$,$2H_2O$ in aqueous solution in the presence of NaCl. Knowing that in conditions of low ionic strengths, electrostatic interactions between macromolecular charges are important [30-33], an electrolyte concentration of 100 mM NaCl was considered to reduce these electrostatic interactions and avoid their influence on turbidity and aggregations studies. Because of this ionic strength, the oberved phenomena occur further in physical level than the chemical one. Batch experiments were carried out by adding variable amounts of metal concentration solution to a given volume of polysaccharide solution. Prior turbidimetric analysis, the polysaccharide/metal mixing was stirred and kept at rest for 16 hours in order to provide information about the formation of soluble or insoluble complexes through colloidal dispersion. On the contrary, in the framwork of aggregation process study, the metal is added to macromolecular solution without mixing action and followed for aggregation evolution after 16 hours at rest.

Methods

Turbidity Measurements. Turbidity measurements were performed with a 2100N Hach Turbidimeter equipped with tungsten filament as the light source. As turbidity values are lower than 40, only one detector located at 90° to the light source carries out the measurement. Above this value, all detectors are used and the turbidity is an average of measurements coming from the three sensors based on the scattered light/transmitted light ratio. For each value of the metal to polymer concentrations ratio examined, several independent suspensions were prepared and runs were performed to ensure the reproducibility of the results. All measurements were carried out at natural pH7 without added reagent and at 25±1 °C.

Light Scattering Measurements. PCS100 Series 4700 spectrometer from Malvern Instruments Ltd was used to follow the aggregation process of CMD suspensions through light Photon Correlation Spectroscopy technique, which enables direct measurements of the dynamic structure by using time correlation functions of the (fluctuating) scattered intensity. PCS100 Series 4700 spectrometer allows to carry out both of static and dynamic light scattering measurements. This equipment is constituted of goniometer mounted on a rotating arm. A laser beam of 514 nm is used as the light source and directed to the sample contained in a quartz cell, which is maintained in the VAT, a calibrated cuvette, implanted in the rotation axis of the spectrometer. A diaphragm controls the amount of scattered light detected and sends it back to the photomultiplier which is sensitive to the quantity of individual photons and allows to fix a diffusion angle ranged from 10° to 150°. Data acquisition were made from a correlator which converts the signal whose processing is carried out by a suitable software « CONTIN » provided by Malvern. Dynamic light scattering measurements were carried out at 90° relative to the incident beam. Concerning static light scattering experiments, particles in the measuring cell pass through the expanded parallel beam. The optical lens focuses the nonscattered light and detectors are positioned in the focal plane at various angular positions. The recorded curves were analyzed to extract the information about the form factor (large angles), which leads to the calculation of the fractal dimension. All measurements were carried out at 25±1 °C and at natural pH of 7 without any addition of reagent.

Results and Discussion

Stability conditions of CMD suspensions

Stability conditions of CMD macromolecule suspensions were investigated through turbidity study. Fig 1 shows the evolution of this feature as a function of molar concentration ratios (M/P), in which P corresponds to the amount of the polymer concentration whereas M indicates the metal concentration. The molar concentration ratios correspond to the situation in which the polymer concentration is fixed (2g/L) and variable amounts of metal concentration solution are added to polymer solution.

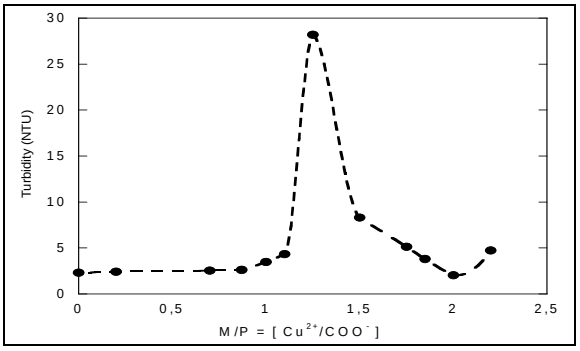

Fig 1: Turbidity profile of CMD suspension as *a* function of the metal to polymer ratios (M/P)

The analysis of the plot exhibits two trends in the range of studied M/P ratios. Firstly, as metal/polymer ratio is increased, the turbidity sharply increases up to a equilibrium point. Then, the turbidity decreases at large metal/polymer ratios. It clearly arises from this turbidity profile that the maximum at 1.25 of M/P is a critical phase change ratio. Below this, turbidity growth is characteristic of slow aggregation, which is accompanied by a formation of stable aggregates even after about 16 h at rest. The photography of suspensions shows no turbid appearence as illustrated in fig 2 (a-c).

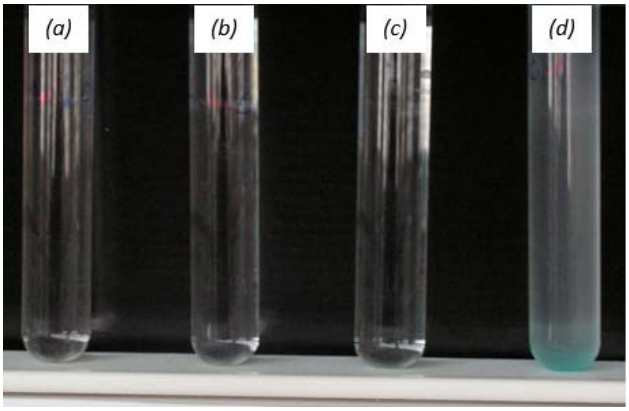

Fig 2: Visual turbidity in 100 mM NaCl at pH7 for 2 g/L CMD in presence of Cu^{2+} with (a) M/P =0, (b) M/P =0.2, (c) M/P = 1, (d) M/P = 2

The situation is different for the area beyond the critical ratio, in which any addition of metal to the suspension leads to a more important aggregation of CMD macromolecules. In this configuration, the metal induces the formation of larger particles and hence a destabilization of these aggregates which will eventually decant. An example of solution is displayed in fig 2 (d), which enables to observe a gelatinous and homogeneous deposit with a bluish coloring due to copper. In order to study the structure of these aggregated particles, the supernatant solution was analysed. This investigation consisted of the determination of their size and fractal dimension.

Aggregats Size of CMD macromolecules in presence of Cu^{2+}

Taking into account previous turbidimetric results, the growth of the mean size clusters was monitored for different M/P ratios located in the areas corresponding to the domain preceding the equilibrum point, then at the equilibrium point (M/P= 1.25) and finally to the domain beyond the peak. In a first step, the behavior of aggregates CMD size was inspected and the fractal dimension of these aggregates was determined in a second step, by knowing that coagulation process depends on the the nature of the interactions, the mobility of objects and the structure of the aggregates. Fig 2 exhibits the distribution of aggregates CMD sizes for M/P ratios of 0.7, 1.25 and 1.75.

By considering the order of magnitude in which the size values are extended, these plots evidence the occurrence of aggregation process in good agreement with the previous turbidity study. For 0.7 corresponding to the lower ratio, a particle size of the order of 50 nm in hydrodynamic diameter is mainly finded, which answers well to the size of the isolated molecules of CMD according to the value summarized in table 1. The wide distribution spread indicates simultaneous formation of two kinds of particles at ratio of 1.25. There are still isolated molecules, but a new strain of clusters of the order of 250 nm appears, which are formed from isolated particles. Then, for these aggregated particles sharply vanish to generate a new strain of more larger aggregates characterized by a diameter of the order of 2300 nm for sufficiently high M/P ratio. To obtain information on the internal structure of these aggregates and the shape of their distribution [34], the angular scattering intensity as a function of scattering angle was recorded and illustrated in fig 3.

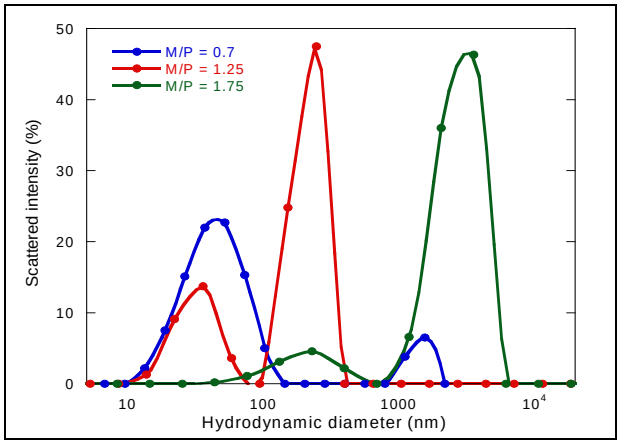

Fig 2. Size distribution of CMD macromolecules in presence of Cu^{2+} for M/P ratios of 0.7 (●), 1.25 (●) and 1.75 (●)

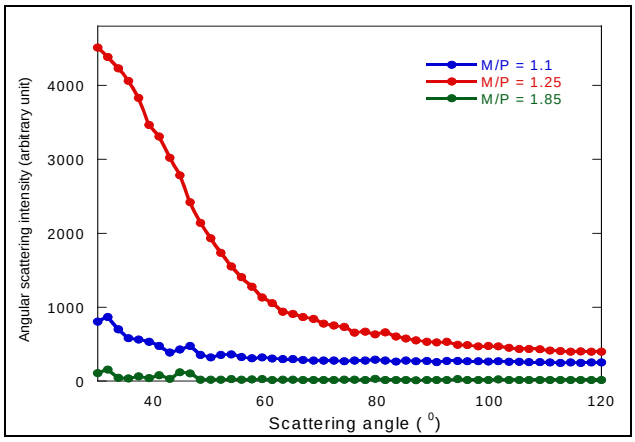

Fig 3 : Angular scattering intensity of as a function of scattering angle for M/P ratios of 1.1 (●), 1.25 (●) and 1.85 (●)

Fractal dimension of aggregates

A comparison of plots shows that the scattered intensity by the aggregated particles is more important for ratio of 1.25 than the data recorded for 1.1. This situation can be explained by aggregates size more larger for the first ratio as above evidenced in dynamic light scattering study. In analogy with this trend, a more scatterd intensity is expected for ratio of 1.85 finding in the area for which aggregates size are the largest, however the intensity is lower than those of both others ratios despite a size that is up to two orders of magnitude greater. This can be explained by the fact that beyond equilibrum ratio of 1.25, decantation of a large part of

the aggregates occurs in good agreement with turbidity data. Fig 4 shows the evolution of fractal dimensions for aggregated particles which were deduced from data recorded in fig 3. In these plots, q is the scattering wave vector, a fundamental characteristic of any scattering process. Its length is expressed acoording to [35] :

$Q = (4\pi n/\lambda)\sin(\theta/2)$,

where n is the refractive index of the medium, λ the light wavelength in the scattering medium and **θ is** the scattering angle (i.e., the angle between the incident beam and the direction of observation).

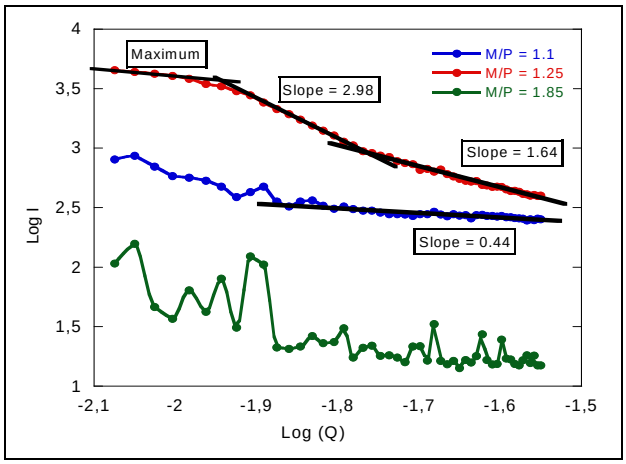

Fig 4 : Log(I) as a function of log(Q) for M/L ratios of 1.1 (●), 1.25 (●) and 1.85 (●)

Whereas the background noise is too large to extract conclusions concerning ratio of 1.85, it may be possible to establish for ratio of 1.1 a slope at the end of the plot. A value of the order of 0.44 is deduced, meaning that there would be a priori high amount of aggregates with a small fractal dimension. In this configuration, the distance between particles is large giving rise to an uncompact structure. This coagulation can be attributed to diffusion limited colloidal aggregation [36-38]. In the case of M/P ratio of 1.25, a closer inspection allow to distinguish various fractal dimensions characterizing the aggregated particles. A first regime for which clusters have a strong compactness whose fractal dimension is in order of 2.98, and a second regime from a strain of aggregates with low compactness of 1.64. There are here two limiting aggregation regimes. The clusters having strong compactness are characterizing by a reaction limited aggregation process [39-41] in opposite to the second regime of particles that are governed by diffusion limited colloidal aggregation. These data are in good agreement with dynamic light scattering results collected at ratio of 1.25 for which hydrodynamic diameter of 120 nm can be attributed to fractal dimension of 2.98 and isolated molecules of 50 nm can assigned to 1.64.

Conclusion

Experimental data evidenced the occurrence of interactions polysaccharides and metals at the supramolecular scale. The stability conditions of the CMD suspensions are characterized by a critical metal / ligand coagulation ratio below which the polymer suspension is stable. Above this ratio, aggregated particles that are formed are suuficiently large to decant and form a gelatinous deposit. It is suitable to study the effect of the formation of this induced polysaccharide deposit around the roots in order to examine whether it is beneficial or not to the phenomena of assimilation of metals by the plant.

References

1. Hąc-Wydro K, Mateja A, Ożóg A, Miśkowiec P. Influence of metal ions on the aggregation of anionic surfactants. Studies on the interactions between environmental pollutants in aqueous solutions. J. Mol. Liq. 2017; 240:514-521.
2. Wuana RA, Okieimen FE. Heavy Metals in Contaminated Soils: A Review of Sources, Chemistry, Risks and Best Available Strategies for Remediation. Int Sch Res Notices Ecology, 2011; Article ID 402647: 20 pages, doi:10.5402/2011/402647.33
3. Zhang F, Yan X, Zeng C, Zhang M, Shrestha S, Devkota LP *et al.* Yao T. Influence of Traffic Activity on Heavy Metal Concentrations of Roadside Farmland Soil in Mountainous Areas. Int J Environ Res Public Health. 2012; 9(5):1715-1731.
4. Buachoon N. Heavy Metal Contamination in Soil and Plant samples by Inductively Coupled Plasma-Optical Emission Spectrometry. Int. J. Chem., Environ. & Biol. Sci. 2014; 2(4):197-200.
5. Sarwar N, Imran M, Shaheen MR, Ishaque W, Hussain S. Phytoremediation strategies for soils contaminated with heavy metals: Modifications and future perspectives Chemosphere. 2017; 171:710-721.
6. Feng NX, Yu J, Zhao HM, Cheng YT, Wong MH. Efficient phytoremediation of organic contaminants in soils using plant-endophyte partnerships, Sci. Total Environ. 2017; 583:352-368.
7. Ali H, Khan E, Sajad MA. Phytoremediation of heavy metals-Concepts and applications. Chemosphere. 2013; 91(7):869-881.
8. Wang H, Zhang H, Cai G. An Application of Phytoremediation to River Pollution Remediation. Procedia Environ. Sci. 2011; 10(C):1904-1907.
9. Pilon-Smits EAH, LeDuc DL. Phytoremediation of selenium using transgenic plants. Curr. Opin. Biotechnol. 2009; 20(2):207-212.
10. Zhanga BY, Zhenga JS, Sharpb RG. Phytoremediation in Engineered Wetlands: Mechanisms and Applications. Procedia Environ. Sci. 2010; 2:1315-1325.
11. Mccutcheon SC, Jorgensen SE. Phytoremediation. Chapter 2, S.E. Jorgensen and B. Fath (ed.), Encyclopedia of Ecology. Elsevier Science BV, Amsterdam, Netherlands. 2008, 2751-2766.
12. Sagou JPS, Rotureau E, Thomas F, Duval JFL. Impact of metallic ions on electrohydrodynamics of soft colloidal polysaccharides. Colloids and Surfaces A: Physicochem. Eng. Aspects. 2013; 435:16-21.
13. Sagou JPS. Electrical Conductivity of Soft Colloidal Polysaccharides: Salt Concentration and Polyelectrolyte Concentration Dependence. Eur. J Sci. Res. 2013; 104(2):230-239.
14. Sagou JPS, Ahualli S, Thomas F. Influence of ionic strength and polyelectrolyte concentration on the electrical conductivity of suspensions of soft colloidal polysaccharides. J. Colloid Interface Sci. 2015; 459:212-217.
15. Peligro FR, Pavlovic I, Rojas R, Barriga C. Removal of heavy metals from simulated wastewater by in situ formation of layered double hydroxides. Chem. Eng. J 2016; 306:1035-1040.

16. Fu F, Wang Q. Removal of heavy metal ions from wastewaters: a review. J. Environ. Manag. 2011; 92:407-418.
17. Zewail TM, Yousef NS. Kinetic study of heavy metal ions removal by ion exchange in batch conical air spouted bed. A.E. J. 2015; 54:83-90.
18. Al-Shannag M, Al-Qodah Z, Bani-Melhem K, Qtaishat MR, Alkasrawi M. Heavy metal ions removal from metal plating wastewater using electrocoagulation: Kinetic study and process performance. Chem. Eng. J. 2015; 260:749-756
19. Alam MM, Alothman ZA, Naushad M, Aouak T. Evaluation of heavy metal kinetics through pyridine based Th(IV) phosphate composite cation exchanger using particle diffusion controlled ion exchange phenomenon. J Ind. Eng. Chem. 2014; 20(2):705-709.
20. Aguado J, Arsuaga JM, Arencibia A, Lindo M, Gascón V. Aqueous heavy metals removal by adsorption on amine-functionalized mesoporous silica. JJ. Hazard. Mater. 2009; 163(1):213-221.
21. SF Lo, SY Wang, MJ Tsai, LD Lin. Adsorption capacity and removal efficiency of heavy metal ions by Moso and Ma bamboo activated carbons. Chem. Eng. Res. Des. 2012; 90(9):1397-1406.
22. Yin N, Wang K, Wang L, Li Z. Amino-functionalized MOFs combining ceramic membrane ultrafiltration for Pb (II) removal. Chem. Eng. J. 2016; 306:619-628.
23. Zhang L, Zhao YH, Bai R. Development of a multifunctional membrane for chromatic warning and enhanced adsorptive removal of heavy metal ions: Application to cadmium. J Membr. Sci. 2011; 379(1-2):69-79.
24. Folens K, Huysman S, Hulle SV, Laing GD. Chemical and economic optimization of the coagulation-flocculation process for silver removal and recovery from industrial wastewater. Sep. Purif. Technol. 2017; 179:145-151.
25. Pio I, Scarlino A, Bloise E, Mele G, Santoro O, Pastore T. *and al.* Efficient removal of low-arsenic concentrations from drinking water by combined coagulation and adsorption processes. Sep. Purif. Technol. 2015; 147:284-291.
26. Rincón GJ, La Motta EJ. Simultaneous removal of oil and grease, and heavy metals from artificial bilge water using electro-coagulation/flotation. J. Environ. Manage. 2014; 144:42-50.
27. López-Maldonado EA, Oropeza-Guzman MT, Jurado-Baizaval JL, Ochoa-Terán A. Coagulation-flocculation mechanisms in wastewater treatment plants through zeta potential measurements. J Hazard. Mater. 279:1-10.
28. Chaubet F, Champion J, Maïga O, Mauray S, Jozefonvicz J. Synthesis and structure-anticoagulant property relationships of functionalized dextrans: CMDBS. Carbohydr. Polym. 1995; 28:145-152.
29. Mauzac M, Josefonvicz J. Anticoagulant activity of dextran derivatives. Part I: Synthesis and characterization, Biomaterials. 1984; 5:301-304.
30. Duval JFL, Van Leeuwen HP. Electrokinetics of diffuse soft interfaces. 1. Limit of low donnan potentials. Langmuir. 2004; 20:10324-10336.
31. Duval JFL. Electrokinetics of diffuse soft interfaces. 2. Analysis based on the nonlinear Poisson–Boltzmann equation. Langmuir. 2005; 21:3247-3258.
32. Duval JFL, Ohshima H. Electrophoresis of diffuse soft particles. Langmuir. 2006; 22:3533-3546.
33. Sagou JPS, Kouassi SS, Andji JYY. Influence of polyeclectrolyte concentration and metallic ions on viscosity of soft colloidal polysaccharides. Int. J Aca. Sci. Res. 2016; 4(4):75-82.
34. Harif T, Adin A. Size and structure evolution of kaoline $Al(OH)_3$ flocs in the electroflocculation process: A study using static light scattering. Water Res. 2011; 45:6195-6206.
35. Lomakin A, Teplow DB, Benedek GB. Quasielastic Light Scattering for Protein Assembly Studies. In: ‘‘*Methods in Molecular Biology*’’. Methods In Moleculer Biology Edit by E. M. Sigurdsson (Humana Press, Totowa, NJ). 2005; 299:153-176.
36. Witten TA, Sander LM. Diffusion-Limited Aggregation, a Kinetic Critical Phenomenon. Phys. Rev. Lett. 1981; 47 (19):1400-1402.
37. Witten TA, Sander LM. Diffusion-limited aggregation. Phys. Rev. B. 1983; 27:5686-5697.
38. Ball RC, Brady RM, Rossi G, Thompson BR. Anisotropy and Cluster Growth by diffusion-limited aggregation. Phys. Rev. Lett. 1985; 55(13):1406-1409.
39. Jullien R, Kolb M. Hierarchical model for chemically limited cluster-cluster aggregation. J Phys. A: Math. Gen. 1984; 17(12):L639.
40. Brown WD, Ball RC. Computer simulation of chemically limited aggregation. J. Phys. A. 1985; 18(9):L517.
41. Ball RC, Weitz DA, Witten TA, Leyvraz F. Universal Gelation, 1st ed, Amsterdam, North Holland, Netherlands, 1984.